Localizing quantal currents along frog neuromuscular junctions

William Van der Kloot and Ligia Araujo Naves

Department of Physiology and Biophysics and Department of Pharmacological Sciences, Health Sciences Center, State University of New York, Stony Brook, NY 11794-8661, USA

1. We spatially localized the origins of quantal currents by recording simultaneously with two intracellular electrodes and employing the prediction of the one-dimensional cable equations that the time integrals of the resulting voltage changes fall off exponentially with distance.

2. Miniature endplate potentials (MEPPs) were more frequent near the centre of the endplate. In contrast to some work using other methods, we did not find MEPPs originating at the margins of the endplate to be strikingly smaller.

3. Spontaneous MEPPs and uniquantal endplate potentials (EPPs) were released over the same length of endplate and with the same relative probabilities at different regions.

4. Nicotinic agonists decreased evoked quantal output, but did not change the length over which uniquantal EPPs were generated. We conclude they do not block nerve conduction in the terminals.

5. Data sets were obtained with an extracellular electrode and two intracellular electrodes. The extracellular electrode was invariably near the centre of the region in which congruous MEPPs appeared to be generated. However, the range in the calculated positions of the synchronous MEPPs was as long as 0·8 mm. Therefore, it may be possible that extracellular electrodes have a longer recording range than commonly assumed.

Katz and his colleagues (summarized in Katz, 1969) showed that acetylcholine is released from the motor nerve as quanta: packets containing thousands of transmitter molecules. The release of a single quantum generates a miniature endplate potential (MEPP). The endplate potential (EPP) is produced by the almost synchronous release of several hundred quanta. There is still disagreement about whether the quanta released spontaneously differ from those released by nerve stimulation. Individual quanta released by nerve stimulation can be observed when the quantal output is drastically decreased by lowering the extracellular concentration of Ca^{2+} and increasing that of Mg^{2+}. Extracellular recording suggests the shapes of the signals generated by evoked and spontaneously released quanta are somewhat different (Cherki-Vakil, Ginsburg & Meiri, 1995). However, when the signals were recorded with the voltage clamp, spontaneous and evoked quanta were indistinguishable (Van der Kloot, 1996). Large & Rang (1978) suggested the false transmitter, acetylmonoethyl-choline, is incorporated more rapidly into quanta released by nerve stimulation than those released spontaneously in the rat (based on a comparison of the decay times of EPPs to extracellular MEPPs). We repeated the experiments on the frog using the voltage clamp and found no evidence for more rapid incorporation into quanta released by stimulation (Naves, Balezina & Van der Kloot, 1996).

An unresolved question that bears on this issue is whether the spontaneous and evoked releases both occur along the entire motor nerve terminal. The frog motor nerve terminal consists of finger-like branches (reviewed by Salpeter, 1987) extending for an appreciable distance. Usually the active zones for vesicle release are distributed all along the branches. To answer this question we experimentally localized the sites at which spontaneous and evoked quantal releases generate depolarizations along the junction, using a method in which signals are recorded with two intracellular electrodes placed on either extremity of the endplate. The site at which a uniquantal signal was generated can be estimated by comparing the voltage–time integrals of the potential changes, $\int V_1$ and $\int V_2$ (Van der Kloot, Madden, Kita & Cohen, 1975).

Other investigators have used two intracellular electrodes to localize events at the endplate, but measured the amplitudes of the signals rather than their time integrals (Gunderson, Katz & Miledi, 1981; Tremblay, Robitaille & Grenon, 1984; D'Alonzo & Grinnell, 1985; Robitaille, Tremblay & Grenon, 1987*a*, *b*; Robitaille & Tremblay, 1989). They did not compare the localization of spontaneous and evoked releases. The validity of their results will be considered in the Discussion.

In addition to estimating where spontaneous and evoked releases occur, we have used our method to address three

additional questions. (1) Does the size of the MEPP vary with the site of generation? D'Alonzo & Grinnell (1985) concluded there is probably little systematic variation in size. Other workers conclude that the MEPPs at the margins of the junctions are smaller (Bieser, Wernig & Zucker, 1984; Robitaille *et al.* 1987*a*, *b*; Robitaille & Tremblay, 1989). (2) Does depressing quantal release with a nicotinic agonist alter where evoked releases occur? (3) How accurately do extracellular electrodes localize quantal releases (Robitaille & Tremblay, 1989; Bennett, Gibson & Robinson, 1995)?

METHODS

The experiments were done on sartorius or cutaneous pectoris muscles from the frog, *Rana pipiens*. The frogs were double pithed in accordance with the policies of the Animal Users Committee of the State University of New York at Stony Brook. Ringer solution contained (mM): NaCl, 120; KCl, 2·0; $CaCl_2$, 2·5; *N*-tris-(hydroxymethyl)methyl-2-aminoethanesulphonic acid–NaOH (Tes), 4·0 at pH 7·4; neostigmine methylsulphate, 0·003. The Ringer solution also contained 31 nM tetrodotoxin (TTX), except when EPPs were being recorded. The hypertonic sodium gluconate solution contained the same constituents except the NaCl was replaced by 200 mM sodium gluconate. The quantal content of EPPs was reduced by lowering the $CaCl_2$ to 0·10–0·16 mM and adding 2·5 mM $MgCl_2$.

The microelectrodes were bevelled, filled with 3 M KCl and selected for low noise (Lederer, Spindler & Eisner, 1979). The extracellular pipettes usually had a DC resistance of about 2 MΩ; intracellular pipettes had resistances of 3–4·5 MΩ. The preparation was observed through a Wild dissecting microscope, the separation between the electrodes was measured with an ocular micrometer at ×50 magnification to the nearest 0·02 mm. Initially MEPPs were recorded using the two channels of an Axoclamp-2A unit (Axon Instruments). The second channel of the Axoclamp-2A has relatively high instrumental noise for this purpose, so most of the measurements were done using the first channel of the Axoclamp for V_1 and an Axon 401 differential input to a CyberAmp 320 signal conditioner (Axon Instruments) for V_2. The bandwidth was 0·1–1000 Hz. When an extracellular electrode was used it was connected to channel 2 of the Axoclamp. The external signal was amplified further with an Axon 2130 differential amplifier. The amplified signals were sent to a ComputerBoards DAS16/300 A/D converter (Mansfield, MA, USA). It can be programmed to store a set number of samples before and after a trigger signal, so the entire time course of the MEPP could be taken in. The trigger was from an FHC (Brunswick, ME, USA) window discriminator. Programming was done in Borland Pascal with subroutines from ComputerBoards.

EPPs were elicited using a suction electrode to stimulate the motor nerve with 80 μs supramaximal, square pulses at 1 Hz. The response to each stimulus was stored, and the data later reviewed to determine the number of 'failures', n_0, in which no quanta were released. They were used to calculate the mean quantal output, m_0; $m_0 = \ln(N/n_0)$, where N is the total number of stimuli (del Castillo & Katz, 1954). From m_0 we used the Poisson distribution to calculate the expected number of multiquantal releases, and discarded this number of the largest EPPs from the set. Consequently, almost all of the responses we used to estimate sites came from uniquantal releases.

Calibration signals were obtained using the built-in calibrator in the Axoclamp and a WPI Omnical 2010 (Sarasota, FL, USA) in the second channel. For measuring the length constant (λ) of the fibre, a −10 to −40 nA square, outward current pulse of 3 ms duration was passed through electrode 1, while the response was recorded with electrode 2. This was first done with the electrodes positioned for recording the activity at the junction. Then the procedure was repeated with electrode 1 inserted at one or more points further away from electrode 2. A single exponential equation was fitted to the points. The excellent fit of the points to the theoretical curve showed that $\int V$ declines exponentially along the muscle cable. The λ was calculated from the exponential equation and varied substantially from preparation to preparation.

Our method for estimating the sites at which the quanta acted was derived from the equations describing the behaviour of a simple R-C cable (Jack, Noble & Tsien, 1975; Van der Kloot *et al.* 1975). Two intracellular electrodes, 1 and 2, were positioned on either side of the junction. They were separated by a distance, d. The voltage–time integrals of the potential changes, $\int V_1$ and $\int V_2$, were measured at both electrodes. When a current flows into the cable at a distance x from electrode 1, then:

$$x = \left(d - \lambda \ln\left(\frac{\int V_1}{\int V_2}\right)\right) \Big/ 2. \quad (1)$$

The voltage–time integral of the signal at its point of origin, V_0, can then be calculated by:

$$\int V_0 = \int V_1 / e^{-x/\lambda}. \quad (2)$$

$\int V_0$ is directly proportional to the total charge that flows across the membrane (Fatt & Katz, 1951). The equivalent circuit for a muscle fibre is more complicated than the parallel resistance and capacity of the simple cable (Adrian & Almers, 1973; Jack *et al.* 1975). However, a numerical model showed that eqns (1) and (2) also apply to the equivalent circuit of a muscle fibre (Van der Kloot & Cohen, 1985).

Estimates of the 95% confidence limits for the observed distributions were made by the Kolmogorov–Smirnov statistic. D_α, the distance on either side of each point in a cumulative distribution, encloses the desired confidence interval, α. For arrays of $n > 50$ or so, a satisfactory approximation is given by:

$$D_\alpha = \sqrt{(-\ln(0{\cdot}5\alpha)/2n)} - 0{\cdot}16693/n \quad (3)$$

(Zar, 1984). The confidence limits are given by $D_\alpha n$, where n is the total number in the array. Note that the confidence limits are for the observed *distribution*, not for individual estimates of position along the endplate. The confidence limits enable us to determine whether or not two distributions are significantly different from one another.

RESULTS

MEPP localization and sizes

Examples of the localization of MEPPs from junctions on the sartorius and the cutaneous pectoris are shown in Fig. 1*A* and *B*, respectively. The data were plotted as a cumulative curve showing the relation between the total number of MEPPs recorded as a function of the calculated distance from electrode 1. The cumulative curve is the basis for the Kolmogorov–Smirnov statistic. The resulting plot appears S-shaped, indicating that there were fewer releases at the margins of the junction than in the middle (see Fig. 2 for data displayed as a histogram). In the example from the sartorius, releases occurred over a distance of roughly 0·6 mm (Fig. 1*A*). The confidence limits for the localization

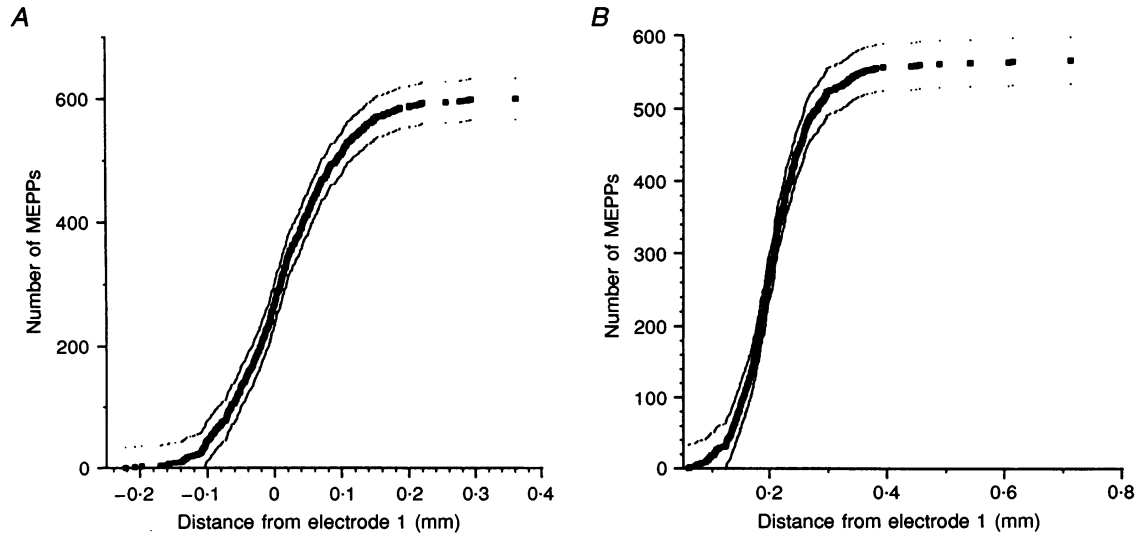

Figure 1. Localization of the estimated sites of MEPP generation on frog muscles

The thin lines on either side of the data points are the ±95% confidence limits. *A*, sartorius: length constant (λ), 1·2 mm; distance between electrodes, 0·26 mm. *B*, cutaneous pectoris: λ, 1·4 mm; distance between electrodes, 0·28 mm.

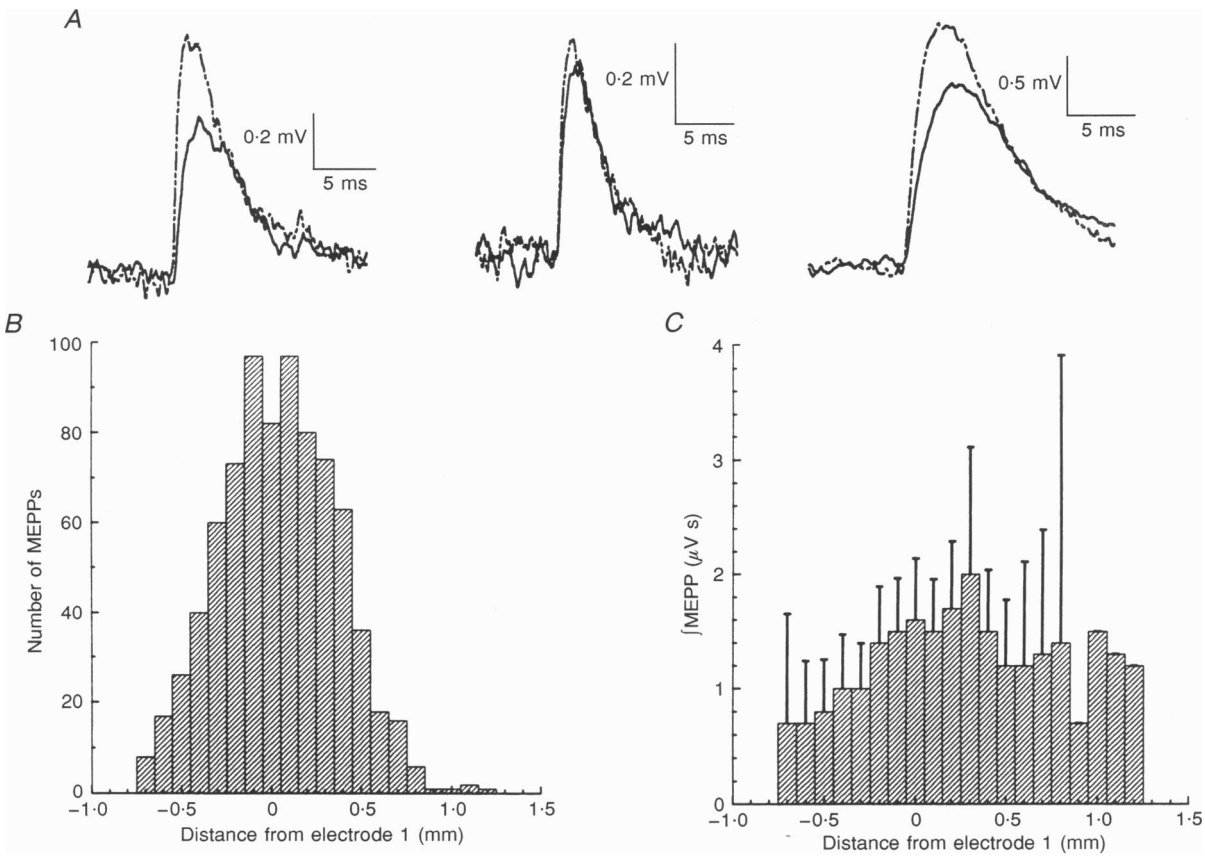

Figure 2. Localization of the sites of MEPP generation and estimates of the sizes of the MEPPs at different points on the endplate of a sartorius muscle (λ = 1·5 mm)

A, examples of the data: continuous line, electrode 1; interrupted line, electrode 2. *B*, a histogram of the distances from electrode 1 to the estimated sites of MEPP generation. *C*, estimates of the calculated $\int V$ measurements at the sites of generation, which are labelled ∫MEPP on the graph. The error bars show the +95% confidence intervals. The four bins on the right had too few members to calculate the confidence interval.

vary with the position on the curve. Near the mid-point of the distribution, the 95% confidence band was 0·03 mm, while at either end of the distribution the confidence bands were more than 0·3 mm. Note that these confidence bands are not for individual estimates of the sites of MEPP generation, they are for the distribution of the cumulative curve of all the localizations. In sartorius junctions, release was spread over a length ranging roughly from 0·2 to 2·0 mm. The patterns of MEPP generation were similar in the cutaneous pectoris (Fig. 1*B*). In the example shown most of the MEPPs were generated over a distance of about 0·4 mm; the confidence limits for the small number of outliers on the right were so broad their apparent location must be interpreted cautiously. In seven data sets from the cutaneous pectoris the longest endplate we encountered was about 0·8 mm.

Figure 2*A* shows examples of MEPPs recorded concurrently with two intracellular electrodes at a sartorius junction. Because the electrodes are inserted away from the centre of the endplate the MEPPs have a low amplitude and rise slowly. Despite our best efforts, there is significant noise on the records, which surely interferes with the accuracy of estimates of localization. The localization of the spontaneous releases at this junction, plotted as a histogram, is shown in Fig. 2*B*. The sizes of the $\int V$ measurements (expressed as ∫MEPP in Fig. 2*C*) at their origins, $\int V_0$, calculated using eqn (2), are plotted as a function of their estimated distances from electrode 1 in Fig. 2*C*, which also shows the 95% confidence limits for the size estimates. Figure 2*C* suggests the ∫MEPPs at either end of the junction are somewhat smaller than those at the centre, but the 95% confidence limits on the individual histogram bins show it is not feasible to distinguish the MEPPs in one bin from those in the neighbouring bin. On the other hand, a single classification analysis of variance (ANOVA) of the bins showed a low probability ($P < 0·001$) that variance was not added due to differences among the heights of the histogram bins. In other words there is a high probability that some of the differences in size along the endplate are statistically significant. However, there is another reason to be sceptical about the reality of a size gradient. The estimate of quantal size at the point of origin depends on the accuracy of the estimate of the distance from the recording electrode (eqn (2)). The confidence intervals for the distance estimates at the margins of the junction are quite broad and consequently the estimates of localization are poor. The imprecision of the position estimates would add to the variance in the size estimates.

To improve our chances of detecting a size gradient, we enlarged the MEPP roughly fourfold by pretreating muscles for 2 h in 200 mM sodium gluconate solution. This increases the amount of acetylcholine per quantum (Van der Kloot, 1987). Figure 3 shows data for 2959 ∫MEPPs recorded from a junction in a preparation pretreated for 2 h in 200 mM sodium gluconate solution (the recordings were done as usual in Ringer solution containing neostigmine and TTX). Some of the MEPPs were extremely large, with peak amplitudes as high as 10 mV. Releases occurred over about 2 mm, and the MEPP frequency was higher near the centre of the junction than at the edges. An examination of the mean ∫MEPP sizes as a function of distance suggests they may be smaller toward the edges, but confidence limits show the difficulty in distinguishing the ∫MEPPs in any one bin from those in the neighbouring bins (Fig. 3*B*). A single classification ANOVA showed the probability was low ($P < 0·001$) that no variance was due to differences in the heights of the bins, so again we cannot rule out the possibility that there are some significant differences in size along the endplate.

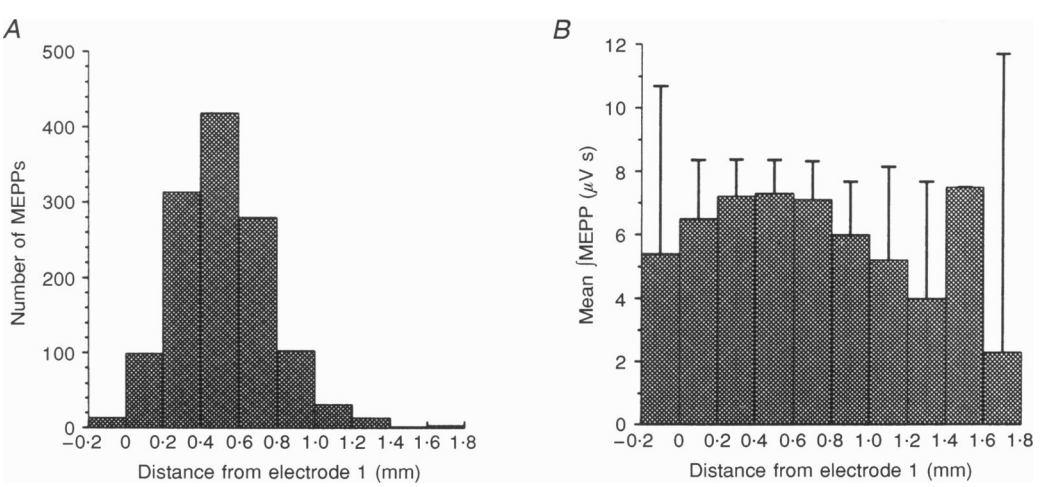

Figure 3. Localization of the sites of MEPP generation and estimates of the sizes of the MEPPs at different points on the endplate of a sodium gluconate-treated sartorius muscle

The sartorius muscle was treated with 200 mM sodium gluconate to enlarge quantal size ($\lambda = 1·8$ mm). *A*, the estimated sites of MEPP generation. *B*, the estimated sizes of the $\int V$ measurements, labelled as ∫MEPP, at the different sites.

The results shown are representative of twelve sets recorded from untreated sartorius preparations and of eight from muscles pretreated in sodium gluconate solution.

Localization of MEPPs and uniquantal EPPs

These experiments were undertaken to see whether spontaneous and evoked releases occur over the same length of junction and whether they occur with similar probabilities from the different parts of the terminal. Using low Ca^{2+}–Mg^{2+} solution, EPPs were recorded, then MEPPs, and in some instances EPPs were recorded once again. Figure 4 shows some of the results plotted as cumulative distributions. The spontaneous and evoked quantal releases occurred over the same length of junction, and the relative probabilities of release from the different points on the nerve terminal were indistinguishable. Four additional experiments (m_0 = 0·62, 0·43, 0·27 and 1·43) led to the same conclusion, namely that there was no statistically significant difference between the distributions of the estimated sites for spontaneous and evoked quantal releases.

Release sites for EPPs when release is depressed by nicotinic agonists

Low concentrations of nicotinic agonists decrease mean quantal release at the frog neuromuscular junction by a mechanism that remains to be explored (Van der Kloot, 1993). One possibility is that nicotinic agonists alter the action potential in the motor nerve terminals, as they do in rat hippocampal neurones (Figenshou, Hu & Storm, 1996). Changes in action potential shape might block their conduction at some nerve terminal branches, reducing the length of terminal available for evoked release. Uniquantal

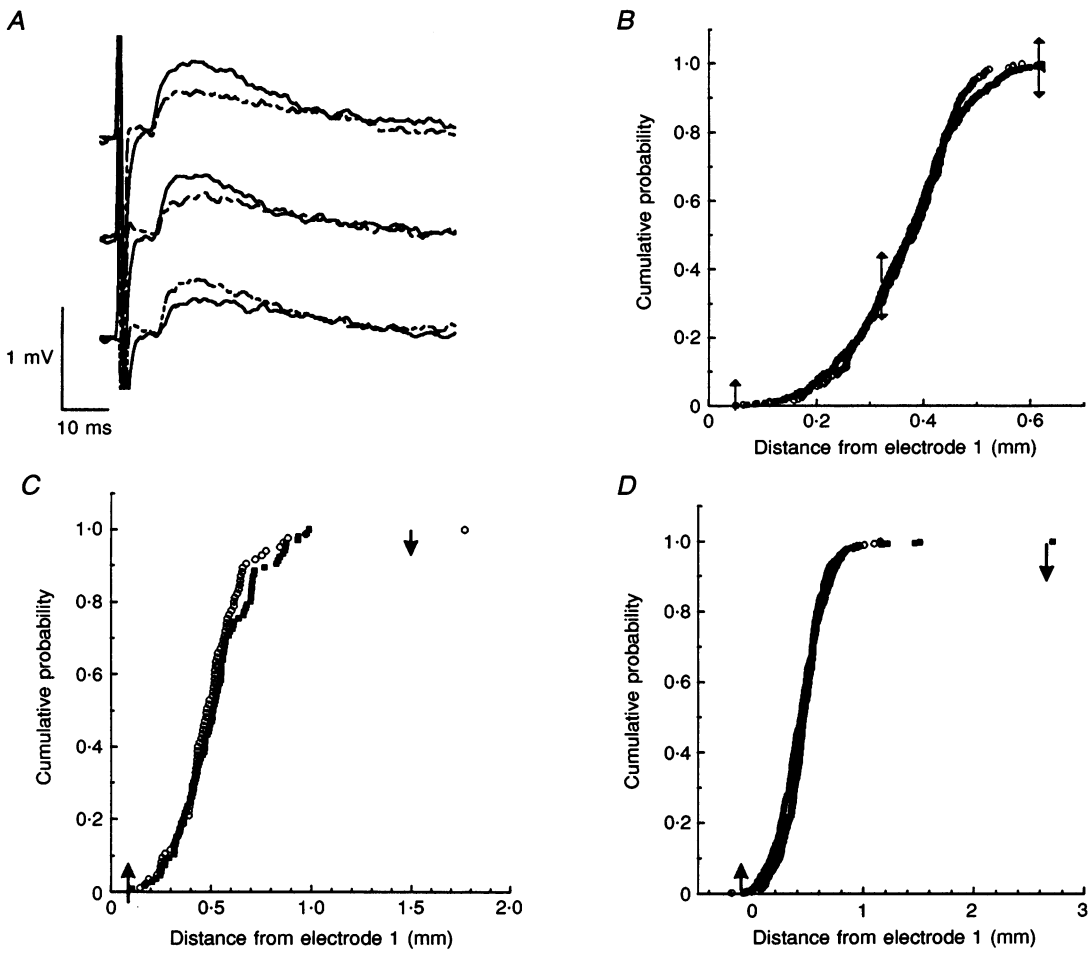

Figure 4. Localization of spontaneous and uniquantal evoked releases

A, three examples of evoked releases; note in the top and middle examples the signal was larger at the right electrode (continuous line), while in the lowest example the signal was larger in the left electrode (interrupted line). In panels *B–D*, ○ denotes the evoked release and ■ represents the spontaneous release. It is almost impossible to distinguish between the symbols in each graph because they overlap, suggesting that the two distributions are very similar. Upward arrows indicate +95% confidence limits; downward arrows indicate −95% confidence limits. *B*, 241 evoked releases, m_0 = 0·29, and 498 spontaneous releases; λ = 0·9 mm and d = 0·64 mm. *C*, 85 uniquantal evoked releases, m_0 = 0·28, and 106 spontaneous releases; λ = 1·5 mm and d = 0·6 mm. *D*, 306 uniquantal evoked releases, m_0 = 0·27, and 453 spontaneous releases; λ = 1·7 mm and d = 0·6 mm. Same data set as the examples in *A*.

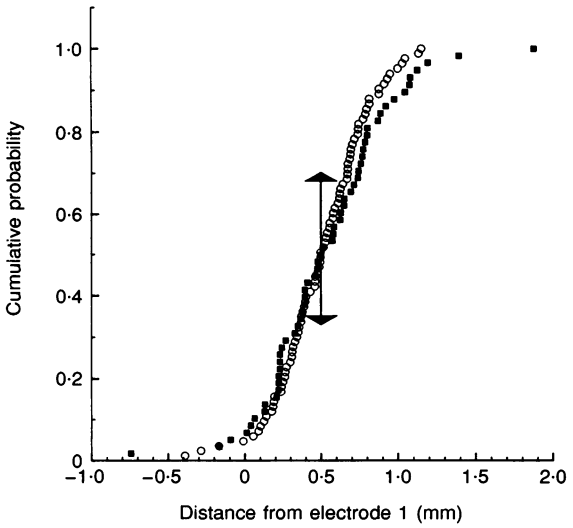

Figure 5. Estimates of the sites of release of uniquantal EPPs before and after carbachol

Estimates before (○) and after the application of 2 μM carbachol (■); $\lambda = 2{\cdot}0$. The arrows show the $\pm 95\%$ confidence limits for the distribution after the application of carbachol.

EPPs were localized at junctions in low Ca^{2+}–Mg^{2+} solution before and after exposure to 2 μM carbachol (Van der Kloot, 1993). In the presence of carbachol, quantal output decreased: in the example shown m_0 fell from 0·33 to 0·15, but the localization of releases was unaltered (Fig. 5). Four additional experiments led to the same conclusion (m_0: 0·19→0·13; 0·40→0·18; 0·66→0·16; and 0·25→0·12).

Localization with both intracellular and extracellular electrodes

A properly positioned extracellular microelectrode detects negative-going signals that are generated by currents flowing into the endplate to generate MEPPs; we will refer to such signals as externals. In these experiments a microelectrode was moved over the surface of a fibre until externals were detected. Then intracellular electrodes were inserted into the same fibre, and MEPPs and externals were simultaneously recorded. Lastly the length constant was determined as usual. Two examples in which relatively small fractions of the MEPPs were synchronous with externals are shown in Fig. 6. The MEPPs accompanied by externals were generated in the region over which the extracellular electrode was positioned. However the regions over which synchronous externals and MEPPs were recorded were quite long, those in Fig. 6*B* extended for almost 0·8 mm. Many of the MEPPs were not accompanied by an external, even when they were estimated to occur at the same region of the junction. This can be explained because often the nerve

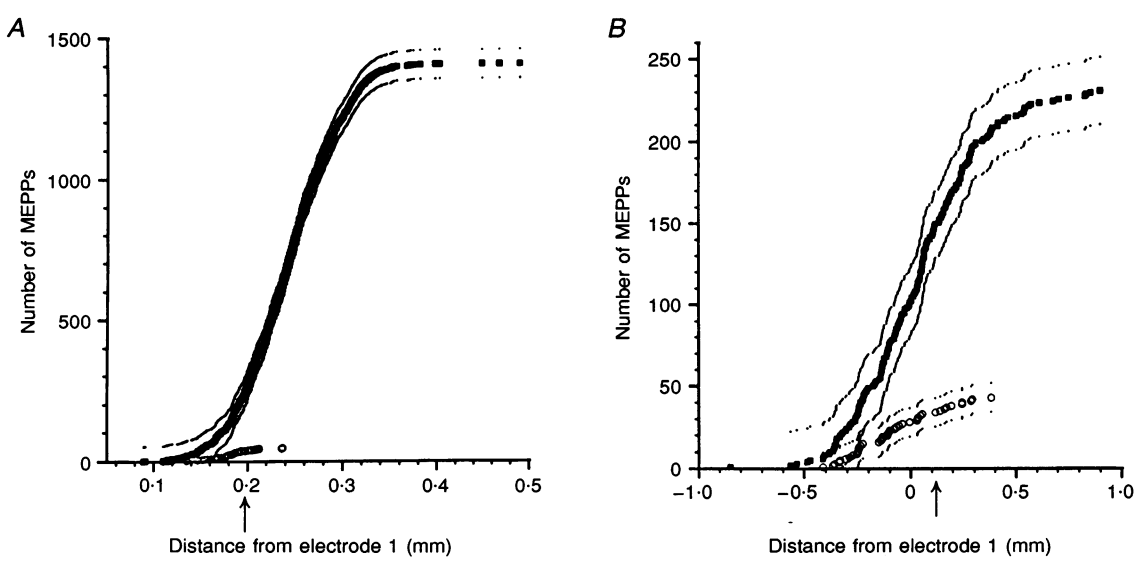

Figure 6. Estimated site of generation of MEPPs accompanied and not accompanied by an external

■, total MEPPs recorded at the junction. ○, MEPPs accompanied by an external. The arrows on the x-axes indicate the position of the extracellular electrode. *A*, $\lambda = 0{\cdot}9$ mm, 3·3% of the MEPPs accompanied by an external. *B*, $\lambda = 1{\cdot}9$, 13·8% of the MEPPs accompanied by an external. The thin lines on either side of the data points are the $\pm 95\%$ confidence limits.

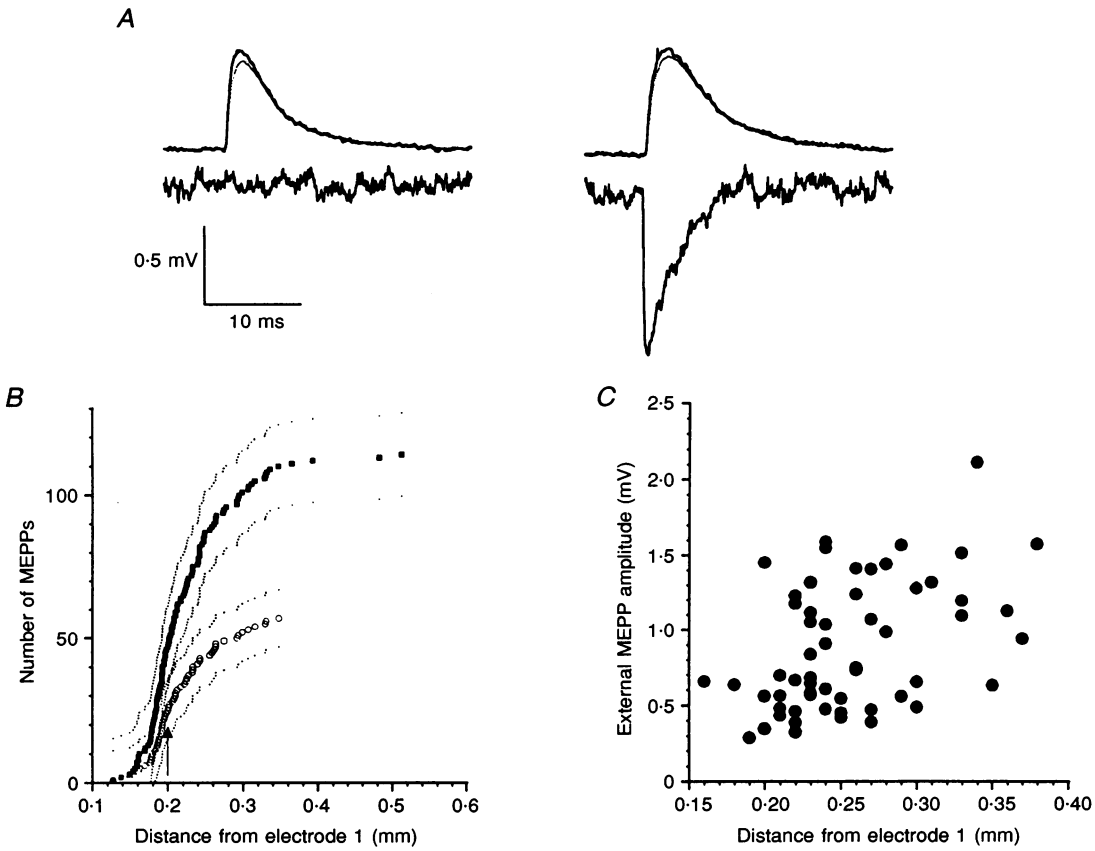

Figure 7. Distribution of MEPPs accompanied by an external at a junction

A, examples of the two intracellular and, beneath them, the extracellular record. The example to the left has no external MEPP, the example on the right has an external MEPP. *B*, distance from electrode 1 of all of the MEPPs recorded at the junction (■); localization of the MEPPs accompanied by an external (○). The arrow on the *x*-axis indicates the position of the extracellular electrode. The dotted lines indicate the confidence limits, as in Fig. 6. *C*, distribution of external sizes as a function of calculated distance.

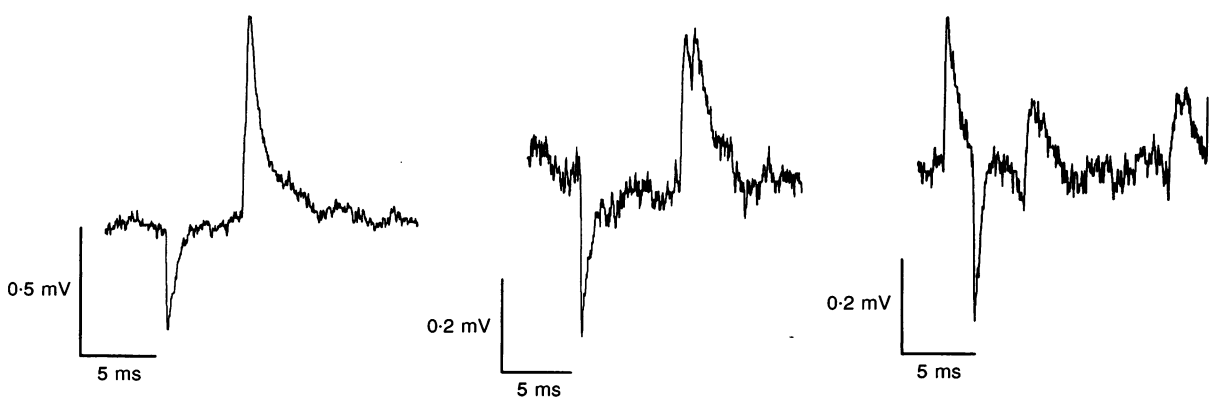

Figure 8. Three examples of recordings with intracellular electrodes that appear to show both MEPPs and externals generated in another fibre

The resting potentials were −85 mV (left panel), −89 mV (centre panel) and −79 mV (right panel).

terminals have several parallel branches. The extracellular electrode might be over one branch, so it would detect releases from this branch but not from the others, even though the branches cover the same length of the muscle fibre. Similar results were obtained in four other examples.

Previous work showed that sometimes a substantial fraction of the MEPPs are accompanied by externals (references in Cohen, Barton & Van der Kloot, 1981). Figure 7 shows the results from a junction where 50% of the MEPPs were synchronous with an external. Note that at this junction most of the releases occurred over a length of about 0·2 mm (Fig. 7*B*); it was one of the shortest lengths for MEPP generation we found on a sartorius muscle. The shortness may account for the high coincidence of externals and MEPPs. The amplitudes of the externals did not appear to be correlated with the site of MEPP generation (Fig. 7*C*). Once again both MEPPs coincident with externals and those without an external appear to come from the same points on the fibre, presumably for the reason presented above.

In some instances when recording with both an intracellular and an extracellular electrode an external is seen that is not accompanied by an MEPP (Cohen *et al.* 1981). Apparently the extracellular electrode detects a miniature generated in an adjacent fibre. Occasionally with an intracellular electrode we record both MEPPs and what appear to be externals from another fibre; three examples are shown in Fig. 8. We cannot readily account for such recordings, but clearly we have much to learn about the equivalent circuit for recording extracellular miniatures.

DISCUSSION

Our methods have two advantages over previous work on the localization of quantal effects. First, our estimates of localization are firmly based on the cable theory, which predicts the integrals of the voltage changes fall off exponentially with distance from the site of current injection. Second, by using appropriate statistical methods we fixed confidence limits for our estimates of the distribution of the sites of quantal generation.

Gunderson *et al.* (1981) recorded MEPP amplitudes with electrodes at either side of the junction. They did not attempt to estimate distances, they compared instead the ratios of the amplitudes of the two signals as an indication of the differences in the sites of generation. D'Alonzo & Grinnell (1985) measured MEPP amplitudes with two intracellular electrodes and assumed the amplitudes decreased exponentially along the fibre (D'Alonzo & Grinnell, 1985). The exponential fall in amplitudes is not predicted by the cable equations and does not occur in model calculations (Van der Kloot & Cohen, 1985), which is why we prefer to use voltage–time integrals. We used the amplitudes from some of our data sets to estimate the sites of generation, calculating an 'amplitude length constant' from the voltage changes produced by the square pulses used to estimate λ. The release sites calculated from the amplitudes alone were invariably spread over a shorter distance than those calculated from the $\int V$ measurements. However, D'Alonzo & Grinnell (1985) calibrated by inserting the current-passing electrode between the two voltage recording sites, while we passed currents at distances greater than those used for the two $\int V$ measurements to provide good data for fitting the exponential decay curve. Their protocol may have increased the reliability of the amplitude method and the correlations they obtained between nerve terminal morphology and estimated site of MEPP generation are impressive.

Other investigators did not measure any length constant (Tremblay *et al.* 1984; Robitaille & Tremblay, 1987, 1989; Robitaille *et al.* 1987*a*, *b*). Instead they inserted their electrodes under visual control at the ends of the terminals and then assumed the highest measured V_1/V_2 was from a release at the end of the terminal closest to electrode 1, the lowest measured V_1/V_2 was from a release close to electrode 2, and that amplitude changed logarithmically between these two points. The assumptions underlying this method are unproven.

Some investigators have concluded the MEPPs are smaller at either extremity of the junction (Bieser *et al.* 1984; Tremblay *et al.* 1984; Robitaille & Tremblay, 1987, 1989; Robitaille *et al.* 1987*a*, *b*). Now others have begun to determine why the sizes are smaller (Anglister, Stiles & Salpeter, 1994). Our results agree with those of D'Alonzo & Grinnell (1985). We do not rule out the possibility that the MEPPs are somewhat smaller at the margins. However even if, on average, these MEPPs are smaller, they overlap in size with the MEPPs recorded from other areas. Consequently, it would be extremely difficult to determine why the sizes are different – if they are different at all.

All workers agree that releases are more frequent at the centre of the terminal than at the ends. The results of D'Alonzo & Grinnell (1985) strongly suggest the frequency of release is proportional to the total length of the nerve terminal.

Our experiments were started because we were interested in whether there were differences between spontaneous and evoked quanta. Spontaneous and uniquantal evoked releases occurred over the same length of fibre, which argues, within the resolution of our method, that they are released from the same sites. Moreover, the normalized cumulative curves for the spontaneous and evoked releases virtually superimpose. Evidently stimulation uniformly elevates the probability of release at all of the sites on the nerve terminal. This agrees with the concept that spontaneous releases are comparable to the spontaneous occurrences of a chemical reaction, while evoked releases correspond to the rate of the same reaction when it is catalysed (Van der Kloot & Molgó, 1994). Bennett, Jones & Lavidis (1986), using

extracellular recording at the toad junction, concluded that release sites near the point of nerve entry contribute most to release. There is no support for this idea from any of the experiments using two intracellular electrodes for localization.

Adding the nicotinic agonist carbachol to the extracellular solution decreases mean evoked quantal output, but does not alter the distribution of sites from which quanta are released. There is no support for the hypothesis that carbachol diminishes evoked release by blocking the action potential before it reaches the ends of the nerve terminals.

The experiments with simultaneous internal and external recording support the idea that the two-electrode method gives reasonable estimates of the site of MEPP generation, because the external electrode was always over the centre of the region in which the synchronous MEPPs were calculated to occur. On the other hand, the calculated positions of the synchronous releases were spread over a considerable length of fibre. Similar spreads were found by Robitaille & Tremblay (1989). There are two opposing interpretations of these results.

The first is that extracellular recordings almost invariably localize release sites within a few micrometres, as is often stated in the literature (for a recent review see Bennett *et al.* 1995). If this is so then much of the apparent spread in the calculated sites of synchronous MEPP generation is due to undetected inaccuracies in our localization method. If the external electrode gives a sharp localization, then we must also conclude that the sites at which the externals are recorded from can have very high release rates; 50% of the total releases can come from a single 'hot spot'. None of the localization experiments have given any indication of the existence of such hot spots. In some cases at least, the external electrode can be moved away and brought close once again without altering MEPP frequency, showing that there was no hot spot due to irritation by the external electrode (Cohen *et al.* 1981). Furthermore, occasionally both MEPPs and what appear to be externals from another fibre are recorded with a single intracellular electrode.

We prefer the alternative interpretation that in at least some cases an external electrode can detect the generation of quanta over a range of tens of micrometres. This could occur if the equivalent circuit for recording miniatures is more complicated than usually assumed (del Castillo & Katz, 1956). One possibility is that the flow of extracellular currents is channelled by the Schwann cells overlying the synaptic cleft (Van der Kloot & Molgó, 1994). Sometimes externals are recorded that are not accompanied by any MEPP, apparently because the external is generated by release on a different fibre (Cohen *et al.* 1981).

Whatever the explanation may be, from the available evidence we think it imprudent to assume an extracellular electrode records only from a sharply circumscribed length of the neuromuscular junction.

Adrian, R. H. & Almers, W. (1973). Measurement of membrane capacity in skeletal muscle. *Nature New Biology* **243**, 62–64.

Anglister, L., Stiles, J. R. & Salpeter, M. M. (1994). Acetylcholinesterase density and turnover number at frog neuromuscular junctions, with modelling of their role in synaptic function. *Neuron* **12**, 783–794.

Bennett, M. R., Gibson, W. G. & Robinson, J. (1995). Probabilistic secretion of quanta: Spontaneous release at active zones of varicosities, boutons, and endplates. *Biophysical Journal* **69**, 42–56.

Bennett, M. R., Jones, P. & Lavidis, N. A. (1986). The probability of quantal secretion along visualized terminal branches at amphibian (*Bufo marinus*) neuromuscular synapses. *Journal of Physiology* **379**, 257–274.

Bieser, A., Wernig, A. & Zucker, H. (1984). Different quantal responses within single frog neuromuscular junctions. *Journal of Physiology* **350**, 401–412.

Cherki-Vakil, R., Ginsburg, S. & Meiri, H. (1995). The difference in shape of spontaneous and uniquantal evoked synaptic potentials in frog muscle. *Journal of Physiology* **482**, 641–650.

Cohen, I. S., Barton, S. B. & Van der Kloot, W. (1981). Bursts of miniature end-plate potentials can be released from localized regions of the frog motor nerve terminal. *Brain Research* **221**, 382–386.

D'Alonzo, A. J. & Grinnell, A. D. (1985). Profiles of evoked release along the length of frog motor nerve terminals. *Journal of Physiology* **359**, 235–258.

del Castillo, J. & Katz, B. (1954). Quantal components of the endplate potential. *Journal of Physiology* **124**, 560–573.

del Castillo, J. & Katz, B. (1956). Localization of active spots within the neuromuscular junction of the frog. *Journal of Physiology* **132**, 630–649.

Fatt, P. & Katz, B. (1951). An analysis of the end-plate potential recorded with an intra-cellular electrode. *Journal of Physiology* **115**, 320–370.

Figenshou, A., Hu, G.-Y. & Storm, J. F. (1996). Cholinergic modulation of the action potential in rat hippocampal neurons. *European Journal of Neuroscience* **8**, 211–219.

Gunderson, C. G., Katz, B. & Miledi, R. (1981). The reduction of end-plate responses by botulinum toxin. *Proceedings of the Royal Society* B **213**, 489–493.

Jack, J. J., Noble, D. & Tsien, R. W. (1975). *Electrical Current Flow in Excitable Cells*, pp. 1–502. Clarendon Press, Oxford, UK.

Katz, B. (1969). *The Release of Neural Transmitter Substances*, pp. 1–60. Liverpool University Press, Liverpool, UK.

Large, W. A. & Rang, H. P. (1978). Factors affecting the rate of incorporation of a false transmitter into mammalian motor nerve terminals. *Journal of Physiology* **285**, 1–24.

Lederer, W. J., Spindler, A. J. & Eisner, D. A. (1979). Thick slurry bevelling. A new technique for bevelling extremely fine microelectrodes and micropipettes. *Pflügers Archiv* **381**, 287–288.

Naves, L. A., Balezina, O. P. & Van der Kloot, W. (1996). Monoethylcholine as a false transmitter precursor at the frog and mouse neuromuscular junctions. *Brain Research* **730**, 58–66.

Robitaille, R. & Tremblay, J. P. (1987). Nonuniform release at the frog neuromuscular junction: evidence of morphological and physiological plasticity. *Brain Research Review* **12**, 95–116.

Robitaille, R. & Tremblay, J. P. (1989). Frequency and amplitude gradients of spontaneous release along the length of the frog neuromuscular junction. *Synapse* **3**, 291–307.

ROBITAILLE, R., TREMBLAY, J. P. & GRENON, G. (1987*a*). Interrelations between MEPP amplitude and MEPP frequency in different regions along the frog neuromuscular junction. *Brain Research* **408**, 353–358.

ROBITAILLE, R., TREMBLAY, J. P. & GRENON, G. (1987*b*). Non-uniform distribution of miniature endplate potential amplitudes along the length of the frog neuromuscular junction. *Neuroscience Letters* **74**, 187–192.

SALPETER, M. M. (1987). Vertebrate neuromuscular junctions: general morphology, molecular organization, and functional consequences. In *The Vertebrate Neuromuscular Junction*, ed. SALPETER, M. M., pp. 1–54. Liss, NY, USA.

TREMBLAY, J. P., ROBITAILLE, R. & GRENON, G. (1984). Distribution of spontaneous releases along the frog neuromuscular junction. *Neuroscience Letters* **51**, 247–252.

VAN DER KLOOT, W. (1987). Pretreatment with hypertonic solutions increases quantal size at the frog neuromuscular junction. *Journal of Neurophysiology* **57**, 1536–1554.

VAN DER KLOOT, W. (1993). Nicotinic agonists antagonize quantal size increases and evoked release at frog neuromuscular junction. *Journal of Physiology* **468**, 567–589.

VAN DER KLOOT, W. (1996). Spontaneous and uniquantal-evoked endplate currents in normal frogs are indistinguishable. *Journal of Physiology* **492**, 155–162.

VAN DER KLOOT, W. & COHEN, I. (1985). Localizing the site of generation of uni-quantal endplate potentials using two intracellular microelectrodes. *Neuroscience Letters* **62**, 57–62.

VAN DER KLOOT, W., MADDEN, K. S., KITA, H. & COHEN, I. S. (1975). A method for localizing the sites of spontaneous acetylcholine release at the frog neuromuscular junction. *Journal of General Physiology* **66**, 16a.

VAN DER KLOOT, W. & MOLGÓ, J. (1994). Quantal acetylcholine release at the vertebrate neuromuscular junction. *Physiological Reviews* **74**, 899–991.

ZAR, J. H. (1984). *Biostatistical Analysis*, pp. 548–549. Prentice Hall, Englewood Cliffs, NJ, USA.

Acknowledgements

This work was supported by grant 10320 from the National Institute of Neurological Disorders and Stroke. We thank Judy Samarel for assistance with the manuscript and Ira S. Cohen and George J. Baldo for discussions.

Author's present address

L. A. Naves: Department of Biochemistry and Immunology, Federal University of Minas Gerais, Belo Horizonte, MG, Brazil.

Author's email address

W. Van der Kloot: wvanderkloot@ccmail.sunysb.edu

Received 7 May 1996; accepted 26 July 1996.